Internal Heat Generation Effect on Free Convection Flow of Power-Law Fluids over A Vertical Plate in Porous Media: VHF/VMF

內部熱源效應對於飽和多孔性介質內幂次律流體流經一垂直平板之自然對流: 可變熱通量/可變質通量

Kuo-Ann Yih*, Chuo-Jeng Huang, Uon-Jien Payne, Ming-Shen Sheu 易國安*, 黃卓初,潘永堅,徐明生

Department of Aircraft Engineering, Air Force Institute of Technology 飛機工程系,空軍航空技術學院

Abstract

The influence of the internal heat generation on coupled heat and mass transfer by the free convection flow of a non-Newtonian fluid over a vertical flat plate embedded in a saturated-porous medium is numerically analyzed. The surface of the vertical flat plate is maintained at variable heat flux and variable mass flux (VHF/VMF). In order to obtain the similarity solution, the internal heat generation is of an exponential decaying form. The transformed governing equations are then solved by Keller box method (KBM). Comparisons with previously published work are performed and excellent agreement is obtained. Numerical data for the dimensionless temperature profile, the dimensionless concentration profile, the local Nusselt number and the local Sherwood number are graphically and tabularly presented for the internal heat generation coefficient A^* , the power-law index of the non-Newtonian fluid n, the exponent of VHF/VMF λ , the buoyancy ratio N, and the Lewis number Le. The physical aspects of the problem are discussed in details.

Keywords: internal heat generation, non-Newtonian fluid free convection, vertical flat plate, porous media, VHF/VMF

摘要

本文以一數值方法分析:內部熱源效應對於飽和多孔性介質內非牛頓流體流經一垂直平板之自然對流熱傳與質傳影響。垂直平板的表面維持於可變熱通量/可變質通量之條件。為了要得到一組相似解,內部熱源形式假設為指數漸減形式。經轉換後的控制方程式則以凱勒盒子法求解之。所得的數值計算結果與早期已刊登發表的論文結果作比較,結果非常吻合。本文數值計算的結果主要以圖形與表格的形式來顯示:內部熱源參數,非牛頓流體之冪次律指標,可變壁溫度/可變壁濃度指數,浮力比,路易士數對無因次溫度分佈、無因次濃度分佈、局部紐塞爾數和局部希爾吾德數之影響。文中的物理現象也詳加討論。

關鍵字: 內部熱源,非牛頓流體自然對流,垂直平板,多孔性介質,可變熱通量/可變質通量

1. Introduction

The convective heat transfer in a saturated porous medium has a number of important applications in geothermal and geophysical engineering. These include nuclear reactor cooling system, extraction of geothermal energy, thermal insulation of buildings, filtration processes and disposal of underground nuclear wastes. Recent books by Nield and Bejan [1], Ingham and Pop [2] and Vafai [3] present a comprehensive account of the available information in the field.

A number of industrially important fluids, including fossil fuels which can saturate underground beds, display the behavior non-Newtonian. The non-linear relationship between shear strain rate and shear stress of non-Newtonian fluids in porous matrix is quite different from that of Newtonian fluids in porous media. In the aspect of pure heat transfer, Mehta and Rao [4], Gorla and Kumari [5], and El-Amin et al. [6] investigated the case of the vertical flat plate. Wang et al. [7] examined the body of arbitrary shape. The case of the vertical cone was considered by Cheng [8].

In the aspect of coupled heat and mass transfer, double-diffusion from a vertical surface in a porous region saturated with a non-Newtonian fluid was studied by Rastogi and Poulikakos [9]. El-Hakiem and El-Amin [10] investigated the mass transfer effects on the non-Newtonian fluids past a vertical plate embedded in a porous medium with non-uniform surface heat flux. Cheng [11] examined the natural convection heat and mass transfer of non-Newtonian power law fluids with yield stress in porous media from a vertical plate with variable wall heat and mass fluxes (VHF/VMF). Soret and Dufour

effects on free convection boundary layers of non-Newtonian power law fluids with yield stress in porous media over a vertical plate with variable wall heat and mass fluxes (VHF/VMF) was examined by Cheng [12].

The effect of internal heat generation is important in several applications that include reactor safety analyses, metal waste form development for spent nuclear fuel, fire and combustion studies, and the storage of radioactive materials. A new class of similarity solutions has obtained for isothermal vertical plate in a semi-infinite quiescent fluid with internal heat generation decaying exponentially by Crepeau and Clarksean [13]. Postelnicu et al. [14] used the model of Crepeau and Clarksean [13] to present free convection boundary-layer over a vertical permeable flat plate in a porous medium with internal heat generation. Mohamed [15] investigated the effect of lateral mass flux on the natural convection boundary layers induced by a heated vertical plate embedded in a saturated porous medium with internal heat generation. Grosan and Pop [16] studied the free convection over vertical flat plate with a variable wall temperature and internal heat generation in a porous medium saturated with a non-Newtonian fluid. Groşan at al. [17] analyzed free convection boundary layer over a vertical cone in a non-Newtonian fluid saturated porous medium with internal heat generation. Bagai and Nishad [18] investigated the free convection in a non-Newtonian fluid along a horizontal plate embedded in porous media with internal heat generation. Chamkha et al. [19] studied effect of suction/injection on free convection along a vertical plate in a nanofluid saturated non-Darcy porous medium with internal heat generation. Very recently,

Yih and Huang [20-22] examined the effect of internal heat generation on free convection heat and mass transfer of non-Newtonian fluids flow over a vertical plate [20], vertical full cone [21], and vertical truncated cone [22] in porous media: VWT/VWC, respectively.

The objective of the present work is to extend the work of Yih and Huang [20] to investigate the internal heat generation effect on coupled heat and mass transfer by the free convection flow of a non-Newtonian fluid over a vertical flat plate embedded in a saturated-porous medium: VHF/VMF. To the best of our knowledge, this problem has not been investigated before. It is assumed that the internal heat generation is of the exponential decaying form. The governing equations have been solved numerically using Keller box method (KBM). The results are obtained for various values of the parameters.

2. Analysis

Let us consider the problem of the influence of the internal heat generation on combined heat and mass free convection flow of non-Newtonian fluids over a vertical flat plate embedded in a fluid-saturated porous medium. Figure 1 shows the flow model and physical coordinate system. The origin of the coordinate system is placed at the leading edge of the vertical flat plate, where x and y are Cartesian coordinates measuring distance along and normal to the surface of vertical flat plate, respectively. In order to obtain the similar solution, we consider the boundary condition of variable heat flux $q_w(x)$ and variable mass flux $m_w(x)$ (VHF/VMF); both the ambient temperature and ambient concentration are T_∞ and C_∞ , respectively.

The variations of fluid properties are limited to density variation that affects the buoyancy force term only. The viscous dissipation effect is neglected for the low velocity. The flow of a non-Newtonian fluid through the porous medium is governed by the power law.

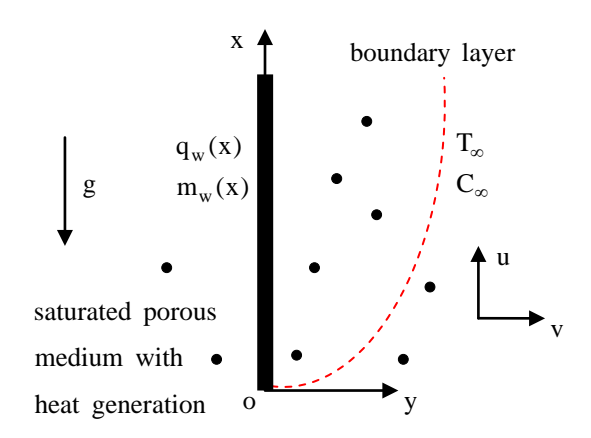


Fig. 1. The flow model and the physical coordinate system

Introducing the boundary layer and Boussinesq approximations, the governing equations and the boundary conditions based on the Darcy law (It is valid under the condition of low velocity and small pores of porous medium [23]) can be written as follows [17, 20]:

Continuity equation:

$$\frac{\partial \mathbf{u}}{\partial \mathbf{x}} + \frac{\partial \mathbf{v}}{\partial \mathbf{y}} = 0,\tag{1}$$

Momentum (Darcy) equation:

$$u^{n} = -\frac{K(n)}{\mu} \left(\frac{\partial p}{\partial x} + \rho g \right), \tag{2}$$

$$v^{n} = -\frac{K(n)}{\mu} \left(\frac{\partial p}{\partial v} \right), \tag{3}$$

Energy equation:

$$u\frac{\partial T}{\partial x} + v\frac{\partial T}{\partial y} = \alpha \frac{\partial^2 T}{\partial y^2} + \frac{q'''}{\rho_{\infty} C_{p}}, \qquad (4)$$

Concentration equation:

$$u\frac{\partial C}{\partial x} + v\frac{\partial C}{\partial y} = D_M \frac{\partial^2 C}{\partial y^2},$$
 (5)

Boussinesq approximation:

$$\rho = \rho_{\infty} \left[1 - \beta_{T} \left(T - T_{\infty} \right) - \beta_{C} \left(C - C_{\infty} \right) \right], \quad (6)$$

Boundary conditions:

$$y = 0$$
: $v = 0$, $-k \frac{\partial T}{\partial y} = q_w(x) = ax^{\lambda}$,
 $-D_M \frac{\partial C}{\partial y} = m_w(x) = bx^{\lambda}$, (7.1-3)

$$y \to \infty$$
: $u = 0$, $T = T_{\infty}$, $C = C_{\infty}$. (8.1-3)

Here, u and v are the Darcian velocities in the x- and y- directions; K(n) is the permeability of the porous medium; n is the power-law index of the non-Newtonian fluid; g is the gravitational acceleration; μ , p and ρ are the viscosity, the pressure and the density of the fluid, respectively; T and C are the volume-averaged temperature and concentration, respectively; α and D_M are the equivalent thermal diffusivity and mass diffusivity, respectively; q" is the internal heat generation rate per unit volume; C_P is the specific heat at constant pressure; β_T and β_C are the thermal and concentration expansion coefficients of the fluid, respectively; k is the equivalent thermal conductivity; a and b are positive constants; λ is the exponent of VHF/VMF; equations (7.2)-(7.3) are the Fourier's law of heat conduction and the Fick's law of mass diffusion, respectively.

The power-law fluid index n for various fluids is as follows:

- (i) n < 1 for pseudo-plastic fluids (for example, the polymer solution) or shear-thinning fluids that have a lower apparent viscosity at higher shear rates.
- (ii) n = 1 for Newtonian fluids (for instance, air and water) where the shear stress is directly proportional to the shear rate.

(iii) n > 1 for dilatant fluids (for example, the suspensions of sand) or shear-thickening fluids for which there is an increase in the apparent viscosity at higher shear rates.

For the power law model of Ostwald-de-Waele, Christopher and Middleman [24] and Dharmadhikari and Kale [25] proposed the following relationships for the permeability of the porous medium:

$$K(n) = \begin{cases} \frac{6}{25} \left(\frac{n\varepsilon}{3n+1}\right)^n \left[\frac{\varepsilon d}{3(1-\varepsilon)}\right]^{n+1} & [24] \\ \frac{2}{\varepsilon} \left[\frac{d\varepsilon^2}{8(1-\varepsilon)}\right]^{n+1} \left(\frac{6n+1}{10n-3}\right) \left(\frac{16}{75}\right)^{\frac{3(10n-3)}{(10n+11)}} & [25] \end{cases}$$

(9)

where d is the particle diameter while ε is the porosity.

The stream function ψ is defined by

$$u = \partial \psi / \partial y$$
, $v = -\partial \psi / \partial x$. (10)

Therefore, the continuity equation is automatically satisfied.

Paying attention to equations (2)-(3). If we do the operation of the cross-differentiation: $\partial(2)/\partial y - \partial(3)/\partial x$, then the pressure terms in equations (2)-(3) can be eliminated. Further, with the help of the equation (6) and the boundary layer approximation $(\partial/\partial x << \partial/\partial y, v << u)$, then we can obtain

$$\frac{\partial u^{n}}{\partial y} = \frac{\rho_{\infty} g K(n)}{\mu} \left(\beta_{T} \frac{\partial T}{\partial y} + \beta_{C} \frac{\partial C}{\partial y} \right). \tag{11}$$

Integrating equation (11) once and with the aid of equation (8), then we get

$$u^{n} = \frac{\rho_{\infty}gK(n)}{\mu} \left[\beta_{T}(T - T_{\infty}) + \beta_{C}(C - C_{\infty})\right] \quad (12)$$

Invoking the following dimensionless variables:

$$\eta = \frac{y}{x} Ra_x^{\frac{1}{2}n+1}$$
 (13.1)

$$f(\eta) = \frac{\Psi}{\alpha R a_x^{1/2_{n+1}}}$$
 (13.2)

$$\theta(\eta) = \frac{(T - T_{\infty}) k Ra_{x}^{\frac{1}{2}n+1}}{q_{w}(x) x}$$
 (13.3)

$$\phi(\eta) = \frac{\left(C - C_{\infty}\right) D_{M} Ra_{x}^{\frac{1}{2}2n+1}}{m_{w}(x) x}$$
 (13.4)

$$Ra_{x} = \frac{\rho_{\infty}g\beta_{T}q_{w}(x)xK(n)}{\mu k} \left(\frac{x}{\alpha}\right)^{n}$$
 (13.5)

where Ra_x is the modified local Rayleigh number for the flow through the porous medium.

In order to achieve the similar solution, the internal heat generation rate per unit volume q''' is modeled according to the following equation [14-22]:

$$q''' = A^* \frac{Ra_x^{\frac{1}{2}n+1} q_w(x)}{x} e^{-\eta}.$$
 (14)

Here, A^* is the internal heat generation coefficient. Note that when $A^* = 0$ corresponds to the case: no internal heat generation (designated as NIHG), however, for $A^* > 0$ corresponds to the other case: with internal heat generation (WIHG).

Substituting equations (13)-(14) into equations (12), (4)-(5), (7)-(8), we obtain

$$(f')^n = \theta + N\phi, \tag{15}$$

$$\theta'' + \frac{n+1+\lambda}{2n+1}f \theta' - \frac{n(1+2\lambda)}{2n+1}f'\theta + A^*e^{-\eta} = 0,$$

(16)

$$\frac{1}{\text{Le}}\phi'' + \frac{n+1+\lambda}{2n+1}f \phi' - \frac{n(1+2\lambda)}{2n+1}f'\phi = 0.$$
 (17)

The boundary conditions are defined as follows:

$$\eta = 0$$
: $f = 0$, $\theta' = -1$, $\phi' = -1$, (18)

$$\eta \to \infty$$
: $\theta = 0, \ \phi = 0.$ (19)

In the above equations, the primes denote differentiation with respect to η . Besides, the buoyancy ratio N and the Lewis number Le are

defined as followed, respectively:

$$N = \frac{\beta_{C} k m_{w}(x)}{\beta_{T} D_{M} q_{w}(x)} = \frac{\beta_{C} k b}{\beta_{T} D_{M} a}, Le = \frac{\alpha}{D_{M}}. (20)$$

In addition, in terms of the new variables, the Darcian velocities in x- and y- directions are, respectively, given by

$$u = \frac{\alpha R a_x^{\frac{2}{2n+1}}}{x} f', \qquad (21)$$

$$v = -\frac{\alpha R a_x^{\frac{1}{2}n+1}}{x} \left[\left(\frac{n+1+\lambda}{2n+1} \right) f - \left(\frac{n-\lambda}{2n+1} \right) \eta f' \right]. \tag{22}$$

The results of practical interest in many applications are both the surface heat and mass transfer rates. The surface heat and mass transfer rates are expressed in terms of the local Nusselt number Nu_x and the local Sherwood number Sh_x respectively, which are basically defined as followed:

$$Nu_{x} = \frac{h_{x}x}{k} = \frac{q_{w}(x) x}{[T_{w}(x) - T_{w}] k}.$$
 (23)

$$Sh_{x} = \frac{h_{m,x}x}{D_{M}} = \frac{m_{w}(x) x}{[C_{w}(x) - C_{m}] D_{M}}.$$
 (24)

where $h_x,\ h_{m,x}$ are the local convective heat transfer coefficient and the local convective mass transfer coefficient, respectively; $q_w(x) = h_x \big[T_w(x) - T_\infty \big]$ (the Newton's law of cooling) and $m_w(x) = h_{m,x} \big[C_w(x) - C_\infty \big]$ (the analogy between the mass transfer and the heat transfer) , respectively.

Inserting equation (13) into equations (23)-(24), the local Nusselt number Nu_x and the local Sherwood number Sh_x in terms of $Ra_x^{\frac{1}{2}n+1}$ are, respectively, obtained by

$$\frac{Nu_x}{Ra_x^{\frac{1}{2}_{n+1}}} = \frac{1}{\theta(0)}, \quad \frac{Sh_x}{Ra_x^{\frac{1}{2}_{n+1}}} = \frac{1}{\phi(0)}.$$
 (25.1-2)

3. Numerical Method

The present analysis integrates the system of equations (15)-(19) by the implicit finite difference approximation together with the modified Keller box method of Cebeci and Bradshaw [26]. To begin with, the differential equations are first converted into a system of five first-order equations. Then these first-order equations are expressed in finite difference forms and solved along with their boundary conditions by an iterative scheme. This approach gives a better rate of convergence and reduces the numerical computational times.

Computations were carried out on a personal computer with the first step size $\Delta\eta_1=0.01$. The variable grid parameter is chosen 1.01 and the value of $\eta_\infty=16$. The iterative procedure is stopped to give the final temperature and concentration distributions when the errors in computing the θ_w and ϕ_w in the next procedure become less than 10^{-5} .

4. Results and Discussion

In order to verify the accuracy of our present method, we have compared our results with those of Hsieh [27], Cheng [11], Yih [28], El-Amin et al. [6], Cheng [12], and Yih [29]. Table 1 illustrates the comparison of the values of $Nu_x/Ra_x^{\frac{1}{2}n+1}$ for various values of λ with n=1, $N=A^*=0$. Table 2 depicts the comparison of the values of $\theta(0)$ for various values of n with n=1 and n=1 and n=1 are n=1 and n=1

Table 1 Comparison of the values of $Nu_x / Ra_x^{\frac{1}{2}n+1}$ for various values of λ with

n =	. 1	N	_	A	* =	0
11 —	· т,	T.A	_	$\boldsymbol{\Gamma}$	_	v

λ	$\operatorname{Nu}_{x}/\operatorname{Ra}_{x}^{\frac{1}{2}n+1}$			
λ	Hsieh [27]	Cheng [11]	Present results	
-0.5	0.5818	0.5818	0.5818	
0.0	0.7715	0.7715	0.7715	
0.5	0.8998	0.8998	0.8998	
1.0	1.0000	1.0000	1.0000	

Table 2 Comparison of the values of $\theta(0)$ for various values of n with $N = \lambda = A^* = 0$

	$\theta(0)$				
n	Yih [28]	El-Amin et	Cheng	Present	
		al. [6]	[12]	results	
0.5	1.3302	1.3294	1.3302	1.3302	
0.8	1.3113		1.3113	1.3114	
1	1.2962	1.2958	1.2962	1.2962	
1.5	1.2641	1.2639	1.2641	1.2641	
2.0	1.2411		1.2411	1.2411	
2.5		_		1.2244	

Table 3 Comparison of the values of $\theta(0)$ for various values of n and λ with $N = A^* = 0$

	$\Theta(0)$				
n	$\lambda = 0$	0.2	$\lambda = 0.5$		
n	El-Amin	Present	El-Amin	Present	
	et al. [6]	results	et al. [6]	results	
0.5	1.2595	1.2643	1.1884	1.1892	
1	1.2083	1.2085	1.1112	1.1114	
1.5	1.1669	1.1670	1.0607	1.0608	
2.0		1.1389	_	1.0279	
2.5	_	1.1191		1.0052	

Table 4 Comparison of the values of $\theta(0)$ and $\phi(0)$ for various values of N and Le with

$n = \lambda = 1, A^* = 0$						
		θ(0)		φ(0)		
N	Le	Yih	Present	Yih	Present	
		[29]	results	[29]	results	
4	1	0.5848	0.5848	0.5848	0.5848	
	10	0.8891	0.8891	0.2172	0.2172	
	100	0.9839	0.9839	0.0747	0.0747	
1	1	0.7937	0.7937	0.7937	0.7937	
	10	0.9635	0.9635	0.2506	0.2507	
	100	0.9955	0.9955	0.0794	0.0795	

The following numerical results are presented for the internal heat generation coefficient A^* ranging from 0 to 1, the power-law index of the non-Newtonian fluid n ranging from 0.5 to 2.0, the exponent of VHF/VMF λ ranging from -0.5 to 1, the buoyancy ratio N ranging from 0 to 10, the Lewis number Le ranging from 0.1 to 10.

The effects of power-law index n and internal heat generation coefficient A^* on the dimensionless temperature and concentration profiles for $\lambda=0$, N=1, Le=2, are shown in Figs. 2 and 3, respectively. In Fig. 2, for the fixed n, it is observed that the dimensionless temperature profile $\theta(\eta)$ increases with increasing the internal heat generation coefficient A^* , thus enhancing the dimensionless wall temperature, i.e., $\theta(0)$; for the fixed A^* , the non-Newtonian fluid with higher power-law index n has the larger dimensionless wall temperature.

Fig. 3 shows that the non-Newtonian fluid with higher power-law index n has larger dimensionless wall concentration, i.e., $\phi(0)$. It is also found that the dimensionless concentration profile $\phi(\eta)$ decreases with increasing the internal heat generation coefficient A*, thus reducing the dimensionless wall concentration.

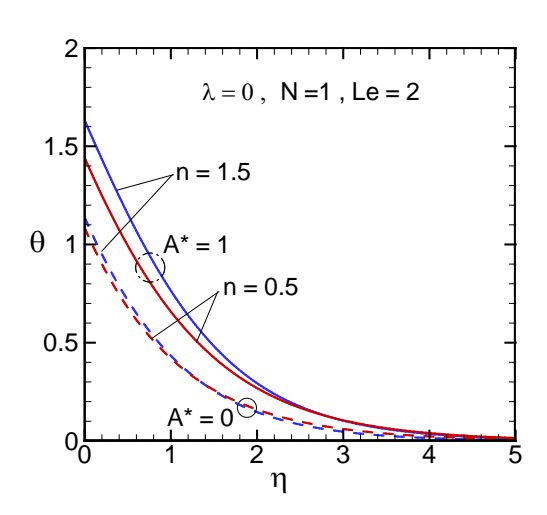


Fig. 2 Effects of power-law index and internal heat generation coefficient on the dimensionless temperature profile

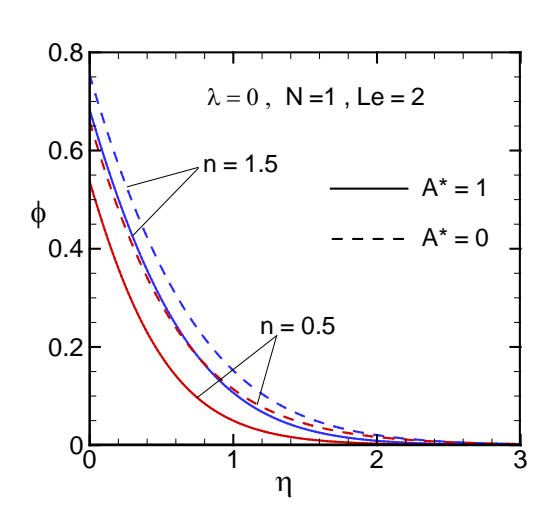


Fig. 3 Effects of power-law index and internal heat generation coefficient on the dimensionless concentration profile

Figs. 4 and 5 illustrate the variation of the local Nusselt number $\frac{Nu_x}{Ra_x^{1/2n+1}}$ and the local Sherwood number $\frac{Sh_x}{Ra_x^{1/2n+1}}$ with the buoyancy ratio N for two values of power-law index (n = 0.5, 1.5) and internal heat generation coefficient (A* = 0,

1) with $\lambda = 0$, Le = 2, respectively. In Fig. 4, on one hand, for fixed n, the local Nusselt number tends to decrease as the internal heat generation coefficient A* is increased. This is because increasing the internal heat generation coefficient A* increases the dimensionless wall temperature $\theta(0)$, as shown in Fig. 2. From equation (25.1), the larger the dimensionless wall temperature, the smaller the local Nusselt number. On the other hand, for fixed A*, the local Nusselt number increases as the power-law index n is decreased. Decreasing the power-law index n tends to increase the velocity of the flow and decrease the dimensionless wall temperature, as shown in Fig. 2, thereby enhancing the local Nusselt number. Thus, the pseudoplastic fluids (n = 0.5) are superior to the dilatant fluids (n = 1.5) from the viewpoint of the free convection heat transfer rates from a vertical flat plate embedded in a porous medium saturated with non-Newtonian power-law fluids. In addition, increasing the buoyancy ratio N tends to increase the buoyancy force, accelerating the flow and thereby increasing the local Nusselt number.

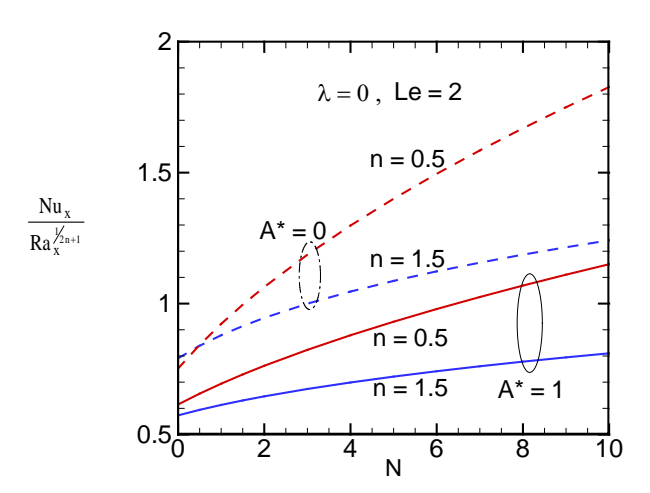


Fig. 4 Effects of power-law index and internal heat generation coefficient on the local Nusselt number

Fig. 5 shows that, for fixed n, the local Sherwood number tends to slightly increase as the internal heat generation coefficient A* is increased. This is because increasing the internal generation coefficient **A*** decreases the dimensionless wall concentration $\phi(0)$, as shown in Fig. 3. From equation (25.2), the thinner the dimensionless wall concentration, the greater the local Sherwood number. For the fixed A*, the local Sherwood number decreases as the power-law index n is increased. Increasing the power-law index n tends to retard the velocity of the flow, thus lowering the local Sherwood number. Thus pseudoplastic fluids (n = 0.5) are superior to the dilatant fluids (n =1.5) from the viewpoint of the mass transfer rates by natural convection from a vertical flat plate embedded in a porous medium saturated with power-law fluids. Besides, enhancing the buoyancy ratio N tends to increase the buoyancy force, accelerating the flow and thereby increasing the local Sherwood number.

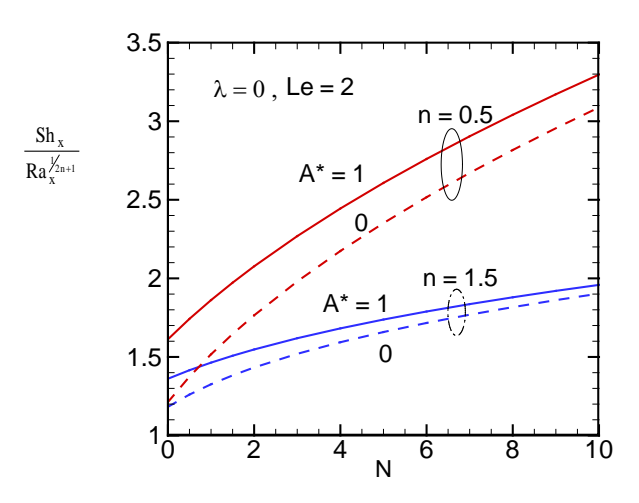
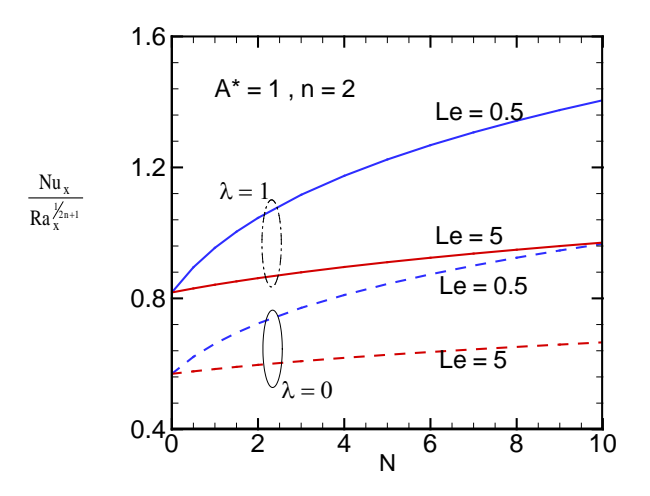


Fig. 5 Effects of power-law index and internal heat generation coefficient on the local Sherwood number

Figs. 6 and 7 show the variation of the local Nusselt number $\frac{Nu_x/Ra_x^{\frac{1}{2}n+1}}{Ra_x^{\frac{1}{2}n+1}}$ and the local Sherwood number $\frac{Sh_x/Ra_x^{\frac{1}{2}n+1}}{Ra_x^{\frac{1}{2}n+1}}$ with the buoyancy ratio N for two values of Lewis numbers (Le = 0.5, 5), exponent of VHF/VMF (λ = 0, 1) with A* = 1, n = 2 respectively. In Fig. 6, comparing these curves

5), exponent of VHF/VMF (λ = 0, 1) with A* = 1, n = 2, respectively. In Fig. 6, comparing these curves, we can find that the local Nusselt number decreases as the Lewis number Le is increased, for fixed N and λ . This is due to the fact that a larger Lewis number Le is associated with a thicker thermal boundary layer. The thicker the thermal boundary layer thickness, the smaller the local Nusselt number. Moreover, for fixed Le, increasing the buoyancy ratio N and the exponent of VHF/VMF λ tends to increase the buoyancy force, accelerating the flow



and thereby increasing the local Nusselt number.

Fig. 6 Effect of the exponent of VHF/VMF and Lewis number on the local Nusselt number

Results in Fig. 7 show that the local Sherwood number increases as the Lewis number Le is increased, for fixed N and $\,^{\lambda}$. This is because that a larger Lewis number Le is associated with a thinner

concentration boundary layer. The thinner the concentration boundary layer thickness, the greater the local Sherwood number. The Lewis number Le has a more significant effect on the local Sherwood number than it does on the local Nusselt number, as compared Figs. 6 and 7. Besides, for fixed Le, increasing the buoyancy ratio N and the exponent of VHF/VMF λ tends to increase the buoyancy force, accelerating the flow and thereby increasing the local Sherwood number.

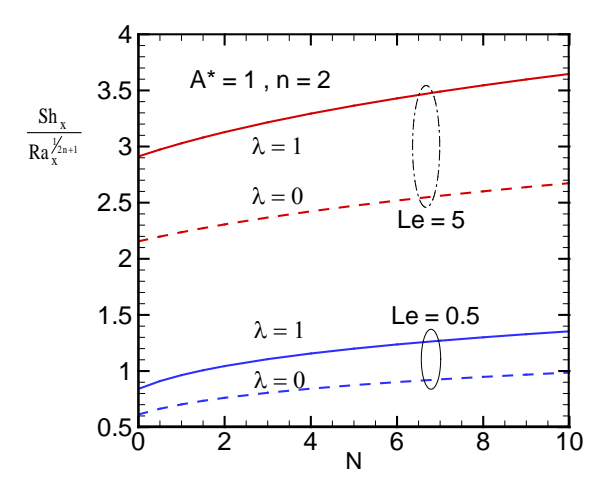


Fig. 7 Effect of the exponent of VHF/VMF and Lewis number on the local Nusselt number

For the sake of future comparison, we illustrated Tables 5-7 and discussed as follows. Table 5 shows the values of $\theta(0)$ for various values of n and λ with N = 0 (pure heat transfer), $A^* = 1$. For the fixed n, the dimensionless wall temperature $\theta(0)$ decreases with increasing the exponent of VHF/VMF λ . For $\lambda \le 0$ ($\lambda = 1$), increasing the power-law index of the non-Newtonian fluid n the enhances (reduces) dimensionless wall temperature $\theta(0)$. However, for $\lambda = 0.5$, the dimensionless wall temperature $\theta(0)$ increases initially, reaches a maximum in the intermediate value of n, and then reduces gradually.

Table 5 Values of $\theta(0)$ for various values of n and λ with N = 0, $A^* = 1$

	θ(0)				
n	$\lambda = -0.5$	$\lambda = 0$	$\lambda = 0.5$	$\lambda = 1$	
0.5	2.0339	1.6269	1.4401	1.3244	
0.8	2.2569	1.6943	1.4495	1.3026	
1	2.3557	1.7170	1.4458	1.2854	
1.5	2.5154	1.7447	1.4303	1.2488	
2.0	2.6105	1.7559	1.4158	1.2223	
2.5	2.6735	1.7612	1.4041	1.2029	

Table 6 shows the values of $\theta(0)$ and $\phi(0)$ for the various values of N, n and A^* with $\lambda=0$, Le = 1, respectively. For the given N and n, increasing the internal heat generation coefficient A^* increases the dimensionless wall temperature $\theta(0)$, but decreases the dimensionless wall concentration $\phi(0)$. It is observed that, for the fixed A^* , both the dimensionless wall temperature $\theta(0)$ and the dimensionless wall concentration $\phi(0)$ reduce as the buoyancy ratio N is increased or the power-law index n is decreased.

Table 6 Values of $\theta(0)$ and $\phi(0)$ for various values of N, n and A* with $\lambda = 0$, Le = 1

N		θ($\theta(0)$		(0)
IN	n	$A^* = 0$	$A^* = 1$	$A^* = 0$	$A^* = 1$
4	0.5	0.5949	0.9122	0.5949	0.5472
	0.8	0.7061	1.0708	0.7061	0.6633
	1	0.7580	1.1472	0.7580	0.7184
	1.5	0.8454	1.2806	0.8454	0.8125
	2.0	0.8995	1.3667	0.8995	0.8716
1	0.5	0.9406	1.3096	0.9406	0.7808
	0.8	1.0045	1.4268	1.0045	0.8726
	1	1.0288	1.4765	1.0288	0.9115
	1.5	1.0630	1.5541	1.0630	0.9717
	2.0	1.0804	1.5988	1.0804	1.0060
0	0.5	1.3302	1.6269	1.3302	0.9653
	0.8	1.3114	1.6943	1.3114	1.0279
	1	1.2962	1.7170	1.2962	1.0508
	1.5	1.2641	1.7447	1.2641	1.0817
	2.0	1.2411	1.7559	1.2411	1.0964

Table 7 illustrates the values of $\theta(0)$ and $\phi(0)$ for the various values of N, Le, λ with $A^* = 1$, n = 2.0, respectively. For the given N and λ , increasing the Lewis number Le increases the dimensionless wall temperature $\theta(0)$, but decreases the dimensionless wall concentration $\phi(0)$. It is found that, for the fixed Le, both the dimensionless wall temperature $\theta(0)$ and the dimensionless wall concentration $\phi(0)$ reduce as the buoyancy ratio N and the exponent of VHF/VMF λ are increased.

Table 7 Values of $\theta(0)$ and $\phi(0)$ for various values of N, Le and λ with $A^* = 1$, n = 2.0

N	T a	θ(0)		φ(0)	
IN	Le	$\lambda = 0$	$\lambda = 1$	$\lambda = 0$	$\lambda = 1$
4	0.1	0.9844	0.6782	2.3359	1.7007
	1	1.3667	0.9419	0.8716	0.6369
	10	1.6756	1.1595	0.2971	0.2188
1	0.1	1.2836	0.8881	2.9925	2.1759
	1	1.5988	1.1077	1.0060	0.7375
	10	1.7319	1.2034	0.3160	0.2335
0	0.1	1.7559	1.2223	4.6973	3.2797
	1	1.7559	1.2223	1.0964	0.8066
	10	1.7559	1.2223	0.3245	0.2403

5. Conclusions

A two-dimensional, steady, laminar boundary layer analysis is presented to study the effect of internal heat generation on natural convection flow resulting from combined heat and mass buoyancy effects of a non-Newtonian fluid adjacent to the vertical flat plate maintained at variable heat flux and variable mass flux (VHF/VMF) in a Darcy porous medium. Numerical solutions are obtained for different values of the internal heat generation coefficient A*, the power-law index n, the exponent

of VHF/VMF λ , the buoyancy ratio N, and the Lewis number Le. The local Nusselt (Sherwood) number tends to decrease (increase) as both the internal heat generation coefficient A^* and the Lewis number Le are increased. Enhancing the buoyancy ratio N and the exponent of VHF/VMF λ tends to increase the local Nusselt number as well as the local Sherwood number. In addition, a decrease in the power-law index n of fluids tends to increase the heat and mass transfer from a vertical flat plate in a porous medium saturated with non-Newtonian power-law fluids.

Nomenclature

- A* internal heat generation coefficient
- a positive constant
- b positive constant
- C concentration
- C_P specific heat at constant pressure
- D_M mass diffusivity
- d particle diameter
- f dimensionless stream function
- g gravitational acceleration
- h_x local convective heat transfer coefficient
- $h_{\scriptscriptstyle m\,x}$ $\,$ local convective mass transfer coefficient
- K(n) permeability of the porous medium
- k equivalent thermal conductivity
- Le Lewis number
- mw local wall mass flux
- N buoyancy ratio
- n power-law index of the non-Newtonian fluid
- Nu_x local Nusselt number
- p pressure
- q" internal heat generation rate per unit volume
- qw local wall heat flux
- Ra_x modified local Rayleigh number
- Sh_x local Sherwood number

- T temperature
- u Darcy velocity in the x-direction
- v Darcy velocity in the y-direction
- x streamwise coordinate
- y transverse coordinate

Greek symbols

- α equivalent thermal diffusivity
- $\beta_{\rm C}$ coefficient of concentration expansion
- β_T coefficient of thermal expansion
- ε porosity
- η similarity variable
- θ dimensionless temperature
- λ exponent of VHF/VMF
- μ viscosity
- ρ density
- φ dimensionless concentration
- w stream function

Subscripts

- w condition at the wall
- ∞ ambient

References

- 1. Nield, D. A., and Bejan, A., Convection in Porous Media, 4th edn., Springer, New York, 2013.
- 2. Ingham, D. B., and Pop, I., Transport Phenomena in Porous Media III, Elsevier, Oxford, 2005.
- 3. Vafai, K., Handbook of Porous Media, 2nd edn., Mercel Dekker, New York, 2005.
- 4. Mehta, K. N., and Rao, K. N., "Buoyancy-induced flow of non-Newtonian fluids in a porous medium past a vertical flat plate with nonuniform surface heat flux," Int. J. Engrg. Sci., Vol. 32, pp. 297-302 (1994).
- 5. Gorla, R. S. R., and Kumari, M., "Nonsimilar solutions for free convection in non-Newtonian

- fluids along a vertical plate in a porous medium," Int. J. Num. Methods Heat Fluid Flow, Vol. 9, pp. 847-859 (1999).
- El-Amin, M. F., El-Hakiem, M. A., and Mansour, M. A., "Effect of viscous dissipation on a power-law fluid over plate embedded in a porous medium," Heat Mass Transfer, Vol. 39, pp. 807-813 (2003).
- Wang, S. C., Chen, C. H., and Yang, Y. T., "Natural convection of non-Newtonian fluids through permeable axisymmetric and two-dimensional bodies in a porous medium," Int. J. Heat Mass Transfer, Vol. 45, pp. 393-408 (2002).
- Cheng, C. Y., "Natural convection heat transfer of non-Newtonian fluids in porous media from a vertical cone under mixed thermal boundary conditions," Int. Commun. Heat Mass Transfer Vol. 36, pp. 693-697 (2009).
- Rastogi, S. K. and Poulikakos, D., "Double-diffusion from a vertical surface in a porous region saturated with a non-Newtonian fluid," Int. J. Heat Mass Transfer, Vol. 38, pp. 935-946 (1995).
- 10. El-Hakiem, M. A., and El-Amin, M. F., "Mass transfer effects on the non-Newtonian fluids past a vertical plate embedded in a porous medium with non-uniform surface heat flux," Heat Mass Transfer, Vol. 37, pp. 293-297 (2001).
- 11. Cheng, C. Y., "Natural convection heat and mass transfer of non-Newtonian power law fluids with yield stress in porous media from a vertical plate with variable wall heat and mass fluxes," Int. Commun. Heat Mass Transfer, Vol. 33, pp. 1156-1164 (2006).
- 12. Cheng, C. Y., "Soret and Dufour effects on free convection boundary layers of non-Newtonian

- power law fluids with yield stress in porous media over a vertical plate with variable wall heat and mass fluxes," Int. Commun. Heat Mass Transfer, Vol. 38, pp. 615-619 (2011).
- Crepeau, J. C., and Clarksean, R., "Similarity solutions of natural convection with internal heat generation," J. Heat Transfer, Vol. 119, pp. 183-185 (1997).
- 14. Postelnicu, A., Grosan, T., and Pop, I., "Free convection boundary-layer over a vertical permeable flat plate in a porous medium with internal heat generation," Int. Commun. Heat Mass Transfer, Vol. 27, pp. 729-738 (2000).
- 15. Mohamed, E. A., "The effect of lateral mass flux on the natural convection boundary layers induced by a heated vertical plate embedded in a saturated porous medium with internal heat generation," Int. J. Thermal Sci., Vol. 46, pp. 157-163 (2007).
- 16. Grosan, T., and Pop, I., "Free convection over vertical flat plate with a variable wall temperature and internal heat generation in a porous medium saturated with a non-Newtonian fluid," Tech. Mech., Vol. 21, pp. 313-318 (2001).
- 17. Groşan, T., Postelnicu, A., and Pop, I., "Free convection boundary layer over a vertical cone in a non-Newtonian fluid saturated porous medium with internal heat generation," Tech. Mech., Vol. 24, pp. 91-104 (2004).
- Bagai, S., and Nishad, C., "Free convection in a non-Newtonian fluid along a horizontal plate embedded in porous media with internal heat generation," Int. Commun. Heat Mass Transfer, Vol. 39, pp. 537-540 (2012).
- 19. Chamkha, A. J., Rashad, A. M., Reddy, C. R., and Murthy, P. V. S. N., "Effect of

- suction/injection on free convection along a vertical plate in a nanofluid saturated non-Darcy porous medium with internal heat generation," Ind. J. Pure Appl. Math., Vol. 45, pp. 321-342 (2014).
- 20. Yih, K. A., and Huang, C. J., "Effect of internal heat generation on free convection heat and mass transfer of non-Newtonian fluids flow over a vertical plate in porous media: VWT/VWC," J. Aero. Astro. Avia., Vol. 47, pp. 115-122 (2015).
- 21. Yih, K. A., and Huang, C. J., "Internal heat generation effect on free convection flow of non-Newtonian fluids over a vertical full cone in porous media: VWT/VWC," 2015 Aero. Tech. Flight Safety Conf. (2015).
- 22. Yih, K. A., and Huang, C. J., "Effect of internal heat generation on free convection flow of non-Newtonian fluids over a vertical truncated cone in porous media: VWT/VWC," J. Air Force Insti. Tech., Vol. 14, pp. 1-18 (2015).
- 23. Hong, J. T., Yamada, Y., and Tien, C. L., "Effects of non-Darcian and non-uniform porosity on vertical plate- natural convection in porous media," J. Heat Transfer, Vol. 109, pp. 356-362 (1987).
- 24. Christopher, R. V., and Middleman, S., "Power-law flow through a packed tube," Ind. Engrg. Chem. Fund., Vol. 4, pp. 424-426 (1965).
- 25. Dharmadhirkari, R. V., and Kale, D. D., "Flow of non-Newtonian fluids through porous media," Chem. Engrg. Sci., Vol. 40, pp. 527-529 (1985).
- Cebeci, T., and Bradshaw, P., Physical and Computational Aspects of Convective Heat Transfer, Springer-Verlag, New York, 1984.

- Hsieh, J. C., Chen, T. S., and Armaly, B. F., "Nonsimilarity solutions for mixed convection from vertical surfaces in porous media," Int. Commun. Heat Mass Transfer, Vol. 36, pp. 1485-1493 (1993).
- 28. Yih, K. A., "Uniform lateral mass flux effect on natural convection of non-Newtonian fluids over a cone in porous media," Int. Commun. Heat Mass Transfer, Vol. 25, pp. 959-968 (1998).
- 29. Yih, K. A., "Coupled heat and mass transfer by free convection over a truncated cone in porous media: VWT/VWC or VHF/VMF," Acta Mech., Vol. 137, pp. 83-97 (1999).

航空技術學院學報 第十五卷 第一期(民國一○五年)